ADVANCED TECHNOLOGIES AND MATERIALS VOL. 48, NO.2 (2023), 61 - 68
DOI: 10.24867/ATM-2023-2-004

Received: 27 October 2023
Revised: 23 November 2023
Accepted: 01 December 2023

Advanced Technologies & Materials

http://journal-atm.org
ISSN: 2620-0325 (print), ISSN: 2620-147X (online)

Original article

On Photonic Implementation of Quantum Computers

Svetomir Simonović*

The Academy of Applied Technical Studies Belgrade, Katarine Ambrozić br.3, Belgrade, Serbia

ABSTRACT

The first section of the work investigates light modes as a means of implementing optical qubits and qudits. The modes considered are polarization mode, path mode, transverse spatial mode, frequency mode, temporal bin-mode and temporal mode. Subsequently, mathematical model of linear optical elements like beam splitters (BS) and phase shifters are deduced and their capability of representing any single qubit optical gate is exposed. Finally Knill, Laflamme and Milburn (KLM) method of using linear optical elements to promote nonlinear operations based on nonlinear (nondeterministic) sign-flip gate (NS) is explained, and designs of two qubits conditional sign flip gate (c-$z_{1/16}$) and CNOT gate, both based on KLM method, are demonstrated. So, universal set of quantum gates based on linear optics is possible.

Key words: *Linear optical elements, Hilbert space, Qubit, Qudit.*

1. INTRODUCTION

The requirements for realizing a quantum computer are astounding: scalable physical qubits—two state quantum systems—that can be well isolated from the environment, but also initialised, measured, and controllably interacted to implement a universal set of quantum logic gates. However, a number of physical implementations are being pursued, including nuclear magnetic resonance (NMR), ion, atom, cavity quantum electrodynamics, solid state, superconducting systems and quantum optics [1, 2, 3].

The invention of the laser in the early 1960's and its subsequent development led to an unprecedented increase in the precision with which light could be produced and controlled, and hence enabled the ability to systematically investigate the quantum properties of optical fields. It was soon realized that quantum optics offered a unique opportunity, not previously available to experimentalists, to test fundamentals of quantum theory and later quantum information science. It is natural, then, to consider quantum optics as a physical platform for quantum computation, [4].

Photonics has a rich history as a platform for fundamental quantum mechanics experiments, [5, 6, 7] and it has developed into a competitive technology for quantum computing and quantum networks as well [8, 9, 10, 11].

The primary advantage of an optical approach to quantum computing is that it would allow quantum logic gates and quantum memory devices to be easily connected together using optical fibers or wave-guides in analogy with the wires of a conventional computer. This affords a type of modularity that is not readily available in other approaches. For example, the transfer of qubits from one location to another in ion-trap or NMR systems is a very complex process, [12].

Another important feature of photonic qubits is their resistance to decoherence, even at room temperature. While photons' limited interaction with the environment is an important advantage over matter systems in this context, it complicates the design of the two-qubit gates crucial for universal quantum computation (any quantum logic circuit

* *Corresponding author's.e-mail: ssimonovic@atssb.edu.rs*

can be realized using a combination of only single-qubit and two-qubit gates, [13].
Qubit is a 2-dimensional quantum system, the state of which is a unit-length vector in complex Hilbert space, [14].
Quantum systems the state of which is a unit-length vector in complex Hilbert space with more than two dimensions are typically called "qudits", [15].
In the case of LOQC, the typical qubit is a photon that can be in one of two modes.
An optical mode is a physical system whose state space consists of superpositions of the number states $|n\rangle$, where n = 0,1,2,… gives the number of photons in the mode (Fock states).
If more than one mode is used, they are distinguished by labels. For example $|k\rangle_r$ is the state with k photons in the mode labeled r. The Hermitian transpose of this state is denoted by ${}^r\langle k|$. The vacuum state for a set of modes has each mode in the state $|0\rangle$ and is denoted by $|\mathbf{0}\rangle$. The annihilation operator for mode r is written as $\hat{a}_r$ and the creation operator as $\hat{a}_r^\dagger = (\hat{a}_r)^\dagger$, where $\hat{a}_r^\dagger|m\rangle = \sqrt{m+1}|m+1\rangle$.
Labels are omitted when no ambiguity results. Hamiltonians that are at most quadratic in creation and annihilation operators generate the group of linear optics transformations. Among these, the ones that preserve the particle number are called passive linear. Every passive linear optics transformation U can be achieved by a combination of beam splitters and phase shifters. If U is passive linear, then $U\hat{a}_r^\dagger|0\rangle = \sum_s u_{sr}\hat{a}_s^\dagger|0\rangle$, where u_{sr} defines a unitary matrix $\hat{u}$. Conversely, for every unitary matrix $\hat{u}$, there is a corresponding passive linear optics transformation. For the remainder of this paper, all linear optics transformations are assumed to be passive, [16].
When several qubits or modes are considered, labels to distinguish between them are used. For example, $|20\rangle_{lm}$ (short for $|2\rangle_l|0\rangle_m$) is a state where modes l and m have two and zero photons, respectively. The basic states of a bosonic qubit encoded in modes l_1 and l_2 are $|\mathbf{0}\rangle \rightarrow |0\rangle_{l_1}|1\rangle_{l_2}$ and $|\mathbf{1}\rangle \rightarrow |1\rangle_{l_1}|0\rangle_{l_2}$, [17].

2. OPTICAL QUBITS IMPLEMENTATIONS

Starting from a very general point of view, light can be deemed as having four degrees of freedom (DOF), any of which could be used to encode quantum information: these are the helicity and the three components of the momentum vector. In a beamlike geometry these may be stated as polarization, transverse mode profile (encompassing two DOFs), and energy (that is, frequency), [15].
With single-rail qubi encoding the vacuum $|0\rangle$ and single-photon $|1\rangle$ states correspond to the logical one and zero, respectively (Fig. 1). Single-rail qubits are however notoriously inconvenient when it comes to quantum information processing and communication by means of light. This is because single-qubit operations are difficult in this encoding. Additionally, the information carried by a single-rail qubit can be easily distorted by optical loss, which results in $|1\rangle$ becoming $|0\rangle$.

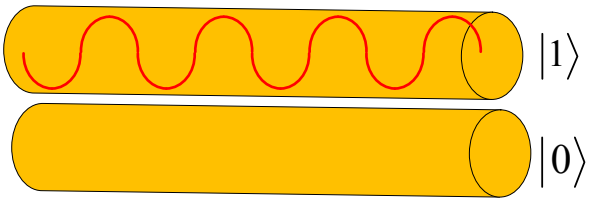

Fig. 1 Single-rail qubit encoding

A much more practical way of encoding the optical qubit is dual-rail (e.g. polarization and path encoding), in which the difference between the logical states consists in the photon occupying one of the two orthogonal optical modes. In this way, the photon is present in any valid state of the qubit, thereby providing an easy way to label loss events, [18].

2.1 Polarization Encoding

In many applications the two qubit modes are the orthogonal polarisation directions, (Fig. 2). This allows easy realisation of single-qubit operations by means of polarisation rotators. In principle, the dual-rail light qubit can be treated as a pair of single-rail qubits carried by each polarisation mode, [18].

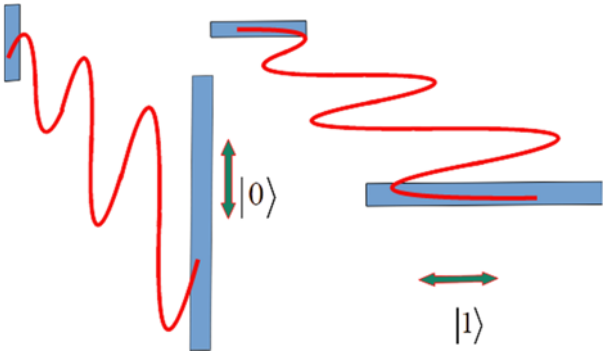

Fig. 2 Polarization based qubits encoding in which a horizontally polarized single photon represents a logical value of 1 and a vertically polarized single photon represents a logical value of 0

2.2 Path Encoding

In path encoding, the value of each qubit is represented by a single photon that may be located in one of two paths, such as two optical fibers (Fig. 3). One path represents a logical value of 0 while the other path represents a value of 1. The logic operations involve interference between different optical paths, which can be very sensitive to thermally-induced phase shifts. The use of polarization-encoded qubits can eliminate the need for any interference between two different optical paths, which may be an advantage in practical applications, [19].

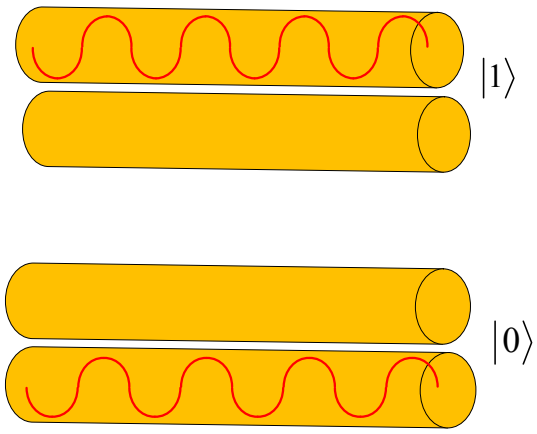

Fig. 3 Path encoding of qubits

2.3 Transverse Spatial Modes Encoding

Transverse mode profile has received considerable attention recently, as it has become apparent that the orbital-angular-momentum (OAM) states of light are a useful basis for encoding information and can be efficiently sorted with time-stationary linear optical elements, [15].

Transverse spatial modes of light beams refer to modess with inhomogeneous amplitude, phase, and polarization distribution at the plane perpendicular to the direction of beam propagation, such as Hermite–Gaussian (HG)/Laguerre–Gaussian (LG)/Bessel modes [16–18], optical vortex modes with a helical phase front carrying orbital angular momentum, and radially/azimuthally polarized vector modes, [20].

A special property of photons is their orbital angular momentum. Quantum mechanically, the orbital angular momentum occurs in discrete steps of $l\hbar$, where l is an in principle unbounded integer that corresponds to the azimuthal structure. Therefore, high-dimensional quantum information can be stored in the orbital angular momentum of single photons. The fundamental property of photons carrying OAM is the presence of the helical phase factor $e^{il\phi}$ where ϕ is the azimuthal coordinate that is in the plane transverse to the propagation direction, [21].

A variety of spatial modes that carry OAM exist, sharing a helical phase factor but differing in their radial structure. The most prominent example, the Laguerre-Gauss mode LG_p^l accurately describes a photon carrying an OAM of $l\hbar$, [21].

The LG mode family is obtained by solving the paraxial wave equation in cylindrical coordinates. The modes form a complete orthonormal set, where the first index l corresponds to the azimuthal structure and the second index p describes the radial profile. These modes have attracted a lot of attention as they are nicely matching the symmetry of most of the optical devices and, more importantly, the azimuthal index l corresponds to an orbital angular momentum (OAM) caused by the twisted phase front $e^{il\phi}$, where ϕ is the angular position ([21], [22]).

Figure 4 shows images of single photons with different OAM values. The defining feature of LG modes is their spatial phase pattern. Specifically, the pattern is a helical phase that wraps around the axis of propagation l times within a wavelength, which results in a phase singularity at the beam center. Thus, the intensity profile of an LG mode shows the typical donut shaped structure. For single photons, the intensity profile gives the probability of detecting a photon at a certain point. If we place a triggered single-photon camera and detect many heralded photons, then the intensity profile of the respective LG mode emerges, which is shown in Figure 4, [21].

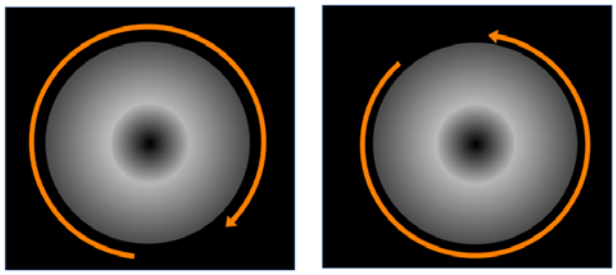

Fig. 4 Frst-order Laguerre-Gauss modes qubits encoding.

2.4 Temporal Modes Encoding

Because frequency and time are conjugate variables, a set of overlapping but orthogonal broadband wave-packet modes are called by the name “temporal modes.” In a coherent-beam-like or single-transversemode guided wave geometry, TMs form a complete basis for representing an arbitrary state in the energy degree of freedom. TMs overlap in time and frequency, yet are field orthogonal. In this respect, they are analogous to transverse spatial modes. Since all TMs “live” inside the same spatial field distribution, they are naturally suited for use with highly efficient and experimentally robust waveguide devices and existing single-mode fiber networks, [15].

Temporal modes (TMs) are orthogonal sets of wave packets that can be used to represent a multimode light field. The mode functions themselves depend on the process and the field is constructed from these functions with weights that are uncorrelated random variables. Because TMs form an orthogonal and complete set, they are also useful for coding information, [23].

For a fixed polarization and transverse field distribution (e.g., in a beamlike geometry), a single-photon quantum state in a specific TM can be expressed as a coherent superposition of a continuum of single-photon states in different monochromatic modes ([15]):

$$|A_j\rangle = \int \frac{d\omega}{2\pi} f_j(\omega)\hat{a}^\dagger(\omega)|0\rangle \qquad (1)$$

Here, $\hat{a}^\dagger(\omega)$ is the standard monochromatic creation operator and $f_j(\omega)$ is the complex spectral amplitude of the wave packet. By Fourier transform, this same state can be expressed as a coherent superposition over many possible “creation times,” and then reads [15].

$$|A_j\rangle = \int \mathrm{d}t \tilde{f}_j(t)\hat{A}^\dagger(t)|0\rangle \quad (2)$$

where

$$\hat{A}^\dagger(t) = \int \frac{d\omega}{2\pi} e^{-l\omega t}\hat{a}^\dagger(\omega)\rangle \quad (3)$$

In Fig. 5, are exemplarily ploted the first two members of a TM basis, chosen for illustration to be a family of Hermite-Gaussian functions of frequency. With this, it is possible to express every single-photon temporal wave-packet quantum state in a basis of TMs as a superposition of wave-packet states,

$$|\Psi\rangle = \sum_{j=1}^{\infty} c_j |A_j\rangle \quad (4)$$

with complex-valued expansion coefficients c_j, [15].

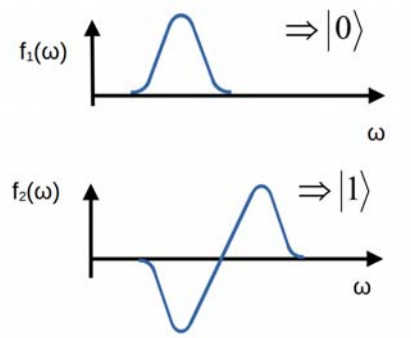

Fig. 5 A Hermite-Gaussian TM qubits encoding basis

TM qudit is defined as a coherent superposition of d TM states:

$$|\Psi\rangle_{TM}^{d} = \sum_{j=0}^{d-1} \alpha_j |A_j\rangle \quad (5)$$

In analogy to this, the definition of a TM qubit requires two orthogonal states with which we associate the logical "0" and "1" , [15].

2.5 *Frequency Modes Encoding*

Frequency mode, termed "spectral LOQC", consists of photonic qubits that occupy two discrete spectral modes. The spectral LOQC Hilbert space consists of a countably infinite set of modes with frequency ω_n, with n any integer. Spatial and polarization degrees of freedom are assumed constant over all frequencies and are neglected. The fixed spacing between modes is $\Delta\omega = \omega_{n+1} - \omega_n$, so that a single dual-rail qubit spanning modes p and q assume the form $|\psi\rangle = \alpha|0\rangle + \beta|1\rangle$, where $|\alpha|^2 + |\beta|^2 = 1$. Here, $|N_p\rangle = (N!)^{-\frac{1}{2}}(\hat{a}_p^\dagger)^N|0\rangle_p$ corresponds to the physical Fock state with N quanta occupying mode p. Figure 6 provides a visualization of this spectral encoding; in this case, a single photon at frequency ω_0 represents$|0\rangle$, whereas a photon at ω_1 signifies $|1\rangle$, [24].

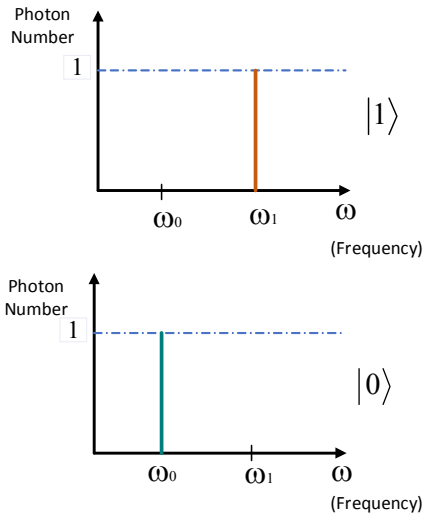

Fig. 6 Spectral qubits encoding basis.

2.6 *Time-bin Modes Encoding*

The time-bin degree of freedom (that is, encoding quantum information in terms of relative arrival times of light pulses) offers a particularly robust kind of single-photon qubits. To understand the basic form of these qubits, consider a single-photon wave packet passing through a two-path Mach-Zehnder interferometer: if the two paths have different lengths, the photon wave packet will exit the interferometer in a quantum-mechanical superposition of an "early time bin" ($|e\rangle$)) and "later time bin ($|l\rangle$)" with a time difference τ_{el} greater than the photon coherence time (Figure 7). By adjusting the parameters of the interferometer to control relative phase and amplitude, one can accurately produce arbitrary time-bin qubits. These time-bin qubits could propagate over long distances in optical fibers with very little decoherence, allowing much more robust quantum communication systems than those based on polarization-encoded qubits, [25].

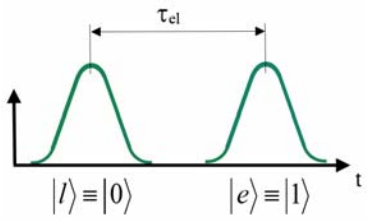

Fig. 7 *A time-bin qubits encoding basis.*

3. SINGLE QUBIT OPTICAL GATES

In quantum optics there are two main parameters in BS, this is its reflection coefficient R (or transmission coefficient T) and phase shift ϕ. Usually, to study the properties of electromagnetic waves (hereinafter referred to as photons) at the output ports of the BS or in technical devices where the BS is a component, in quantum optics it is considered that R and ϕ are constant values.

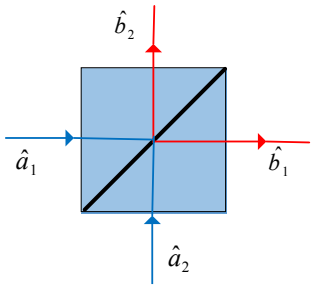

Fig. 8 Beam splitter

Lossless two-mode BS (with two input and output ports, as in Fig. 8) in quantum optics is described by the unitary matrix U_{BS}, which has the form ([26], [27], [28], [29])

$$\begin{pmatrix}\hat{b}_1\\ \hat{b}_2\end{pmatrix} = U_{BS}\begin{pmatrix}\hat{a}_1\\ \hat{a}_2\end{pmatrix} \tag{6}$$

where

$$U_{BS} = \begin{pmatrix}\sqrt{T} & e^{i\phi}\sqrt{R}\\ -e^{-i\phi}\sqrt{R} & \sqrt{T}\end{pmatrix} \tag{7}$$

and the 1st and 2nd mode annihilation operators at BS input are respectively represented by $\hat{a}_1$ and $\hat{a}_2$ and at the BS output ports by $\hat{b}_1$ and $\hat{b}_2$; T and R are the transmittance and reflectance, respectively ($R + T = 1$), and ϕ is the phase shift. In the literature the BS matrix U_{BS} *is used* in various representations. The most commonly used representation is when the phase shift $\phi = \pm\pi/2$, the second representation often encountered is when $\phi = 0$, in these cases the U_{BS} matrix is respectively

$$U_{BS} = \begin{pmatrix}\sqrt{T} & \pm i\sqrt{R}\\ \pm i\sqrt{R} & \sqrt{T}\end{pmatrix} \tag{8}$$

and

$$U_{BS} = \begin{pmatrix}\sqrt{T} & \sqrt{R}\\ -\sqrt{R} & \sqrt{T}\end{pmatrix} \tag{9}$$

Both representations can only be used when the result is independent of the phase shift ϕ.

When the beam splitter is considered in general terms without defining its type, the problem is posed to find the matrix U_{BS} on the basis of general physical considerations. The result has essentially always been the same - this BS matrix has been obtained in Equation (7), (27-29]. Disregarding the effects of polarization, misalignment and imperfect beam collimation, the input annihilation operators $\hat{a}_1$ and $\hat{a}_2$ and output annihilation operators $\hat{b}_1$ and $\hat{b}_2$ at some chosen frequency for linear BS, can be represented as

$$\begin{pmatrix}\hat{b}_1\\ \hat{b}_2\end{pmatrix} = \begin{pmatrix}u_{1,1} & u_{1,2}\\ u_{2,1} & u_{2,2}\end{pmatrix}\begin{pmatrix}\hat{a}_1\\ \hat{a}_2\end{pmatrix} \tag{10}$$

Representation as in Equation (10) is a direct consequence of the conservation of particles (photons) before and after their passage through BS. If photons before hitting the BS were $s_1 + s_2$ and after passing through the BS became $n + m$, then for the number of photons to be conserved $s_1 + s_2 = n + m$ requires that the transformation matrix be in the form of Equation (10), ([28], [30]). The conversion matrix U_{BS} contains the elements $u_{i,j}$ (i, j = 1, 2), which are generally complex and must be represented as

$$u_{i,j} = |u_{i,j}|e^{-i\phi_{ij}} \quad \text{i,j} = 1,2 \tag{11}$$

The well-known bosonic commutation relations at the output of the BS must also hold, i.e.:

$$[\hat{b}_\text{i}, \hat{b}_j^\dagger] = \delta_{i,j} \tag{12}$$

This commutation relation leads to the relations:

$$|u_{1,1}|^2 + |u_{1,2}|^2 = 1\ ; \tag{14}$$
$$|u_{2,1}|^2 + |u_{2,2}|^2 = 1; \tag{15}$$
$$u_{1,1}u_{2,1}^* + u_{1,2}u_{2,2}^* = 0 \tag{16}$$

which further leads to:

$$\theta = arcos\left(T^{\frac{1}{2}}\right), \quad 0 \le \theta \le \pi/2 \tag{17}$$
$$|u_{1,1}|^2 = |u_{2,2}|^2 = T = cos^2\theta \tag{18}$$
$$|u_{1,2}|^2 = |u_{2,1}|^2 = R = sin^2\theta \tag{19}$$

The four-phase dependence can be reduced to a two-phase dependence by making phase substitutions in the form:

$$\phi_\tau = 1/2(\phi_{11} - \phi_{22}); \tag{20}$$
$$\phi_\rho = 1/2(\phi_{12} - \phi_{21} \mp \pi); \tag{21}$$
$$\phi_0 = 1/2(\phi_{11} + \phi_{22}). \tag{22}$$

In this case, the BS matrix Equation (10) will be

$$U_{BS} = e^{-i\phi_0}\begin{pmatrix}e^{i\phi_\tau}cos\theta & e^{i\phi_\rho}sin\theta\\ -e^{-i\phi_\rho}sin\theta & e^{-i\phi_\tau}cos\theta\end{pmatrix} \tag{23}$$

Equation (23) only has two phases left, since ϕ_0 is the phase multiplier, which is known to be negligible. It can be seen that by using the BS matrix in the form of Equation (23), the operators $\hat{b}_1$ and $\hat{b}_2$ can be further simplified, so, it is obtained:

$$\hat{b}_1 = e^{i\phi_\tau}\left(\hat{a}_1 cos\theta + \hat{a}_2 e^{i(\phi_\rho - \phi_\tau)}sin\theta\right) \tag{24}$$
$$\hat{b}_2 = e^{-i\phi_\tau}\left(-\hat{a}_1 e^{-i(\phi_\rho - \phi_\tau)}sin\theta + \hat{a}_2 cos\theta\right) \tag{25}$$

Again the irrelevant phase multipliers in front of the brackets is obtained, which can be disregarded. Introducing the notion of phase difference $\phi = \phi_\rho - \phi_\tau$, the BS matrix U_{BS} is obtained in the form of Equation (7).

So, the unitary matrix associated with a beam splitter with parameters θ, ϕ is:

$$U_{BS}(\theta,\phi) = \begin{pmatrix} cos\theta & e^{i\phi}sin\theta \\ -e^{-i\phi}sin\theta & cos\theta \end{pmatrix} \quad (26)$$

where θ and ϕ are determined by the reflection amplitude R and the transmission amplitude T.
For a symmetric beam splitter, which has a phase shift $\phi = \frac{\pi}{2}$ under the unitary transformation condition, it can be shown that:

$$U_{BS}\left(\theta, \phi = \frac{\pi}{2}\right) = \begin{pmatrix} cos\theta & isin\theta \\ isin\theta & cos\theta \end{pmatrix} = \\ = (cos\theta)I + (isin\theta)\sigma_x = e^{i\theta\sigma_x} \quad (27)$$

which represents a rotation of the single qubit state about the x-axis by 2θ in the Bloch sphere (Fig. 9).
A mirror is a special case where the reflecting rate is 1, so that the corresponding unitary operator is a rotation matrix given by

$$R(\theta) = \begin{pmatrix} cos\theta & -sin\theta \\ sin\theta & cos\theta \end{pmatrix} \quad (28)$$

Similarly, a phase shifter operator associates with a unitary operator P_ϕ described by $U(P_\phi) = e^{-i\phi}$, or, if written in a 2-mode format

$$U(P_\phi) = \begin{pmatrix} e^{-i\phi} & 0 \\ 0 & 1 \end{pmatrix} = e^{-i\frac{\phi}{2}} \begin{pmatrix} e^{-i\frac{\phi}{2}} & 0 \\ 0 & e^{i\frac{\phi}{2}} \end{pmatrix} \approx \\ \left(e^{-i\frac{\phi}{2}}\, ignored\right) e^{-i\frac{\phi}{2}\sigma_z} \quad (29)$$

which is equivalent to a rotation of ϕ about the z-axis (see Fig. 9).

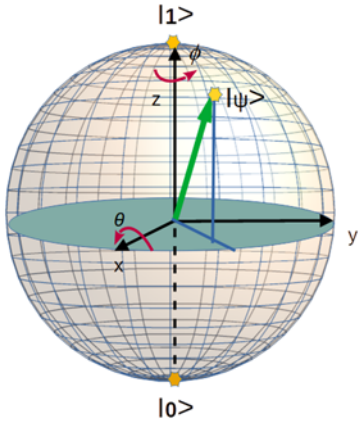

Fig. 9 Bloch sphere representation of a qubit |Ψ⟩

Since any two rotations along orthogonal rotating axes in the Bloch sphere (Fig. 9) can determine arbitrary unit vector, one can use a set of symmetric beam splitters and phase shifters to realize an arbitrary single qubit optical gate.

4 TWO QUBIT OPTICAL GATES

In order to enable two qubit gates optical implementation Knill, Laflamme and Milburn (KLM) used linear optical elements to promote nonlinear operations based on nonlinear sign-flip gate (NS), [17].
The nonlinear sign gate can be implemented non-deterministically by three beam splitters, two photo-detectors, and one ancilla photon (Fig. 10).

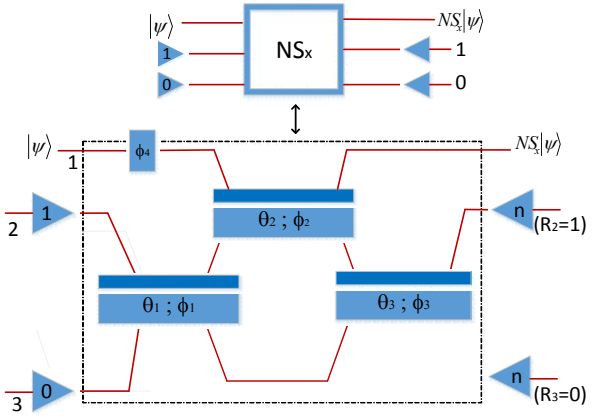

Fig. 10 Linear optics implementation of Nondeterministic Sign-Flip gate (NS-gate). The elements framed in the box (dashed border) are the linear optics implementation with three beam splitters and one phase shifter. Modes 2 and 3 are ancilla modes, and R_2 and R_3 are photon detectors. Adapted from [31], [17].

The NS-gate in Fig. 10 gives a nonlinear phase shift on one mode conditioned on two ancilla modes. The output is accepted only if there is one photon in mode 2 and zero photons in mode 3 detected, where the ancilla modes 2 and 3 are prepared as the $|10\rangle_{2,3}$ state, [31].
The subscript x in the top diagram is the phase shift applied and depends on the choice of phases in the optical elements.
NS gate operates as follows: When a superposition of the vacuum state $|0\rangle$, one photon state $|1\rangle$ and two-photon state $|2\rangle$ is input into the NS gate, the gate flips the sign (or phase) of the probability amplitude of the $|2\rangle$ component, that is a nonlinear sign-flip gate (NS) implements the transform NS:

$$\alpha_0|0\rangle + \alpha_1|1\rangle + \alpha_2|2\rangle \longrightarrow \alpha_0|0\rangle + \alpha_1|1\rangle - \alpha_2|2\rangle \quad (30)$$

which is the basis, along with ancilla, for implementing the two qubits conditional sign flip gate or CNOT-gate, [31].
It should be noted that this operation is nondeterministic because it succeeds with probability $P = \frac{1}{4}$; however the gate always gives a signal (photon detection at R_2 and R_3) when operation is successful, [32].
The implementation of conditional sign flip gate (c-$z_{1/16}$ gate) is made by the combination of the nonlinear sign gate and the physics of Hong-Ou Mandel (HOM) interferometer (Fig. 11).

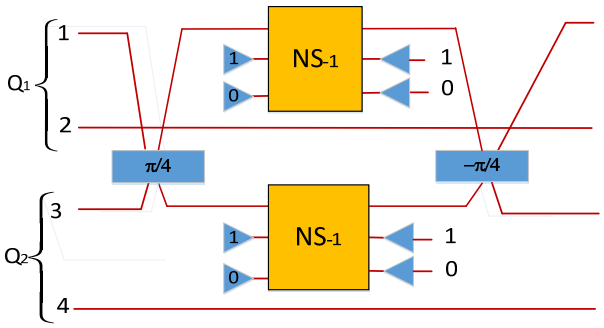

Fig. 11. Conditional sign flip implemented with NS operations. Adapted from [31], [17].

Q_1 and Q_2 refer to arbitrary bosonic qubits encoded in modes 1, 2, and 3, 4, respectively:

$$|Q_1\rangle = \alpha_0|0\rangle_L + \alpha_1|1\rangle_L = \alpha_0|0\rangle_1|1\rangle_2 + \alpha_1|1\rangle_1|0\rangle_2 \quad (31)$$

$$|Q_2\rangle = \alpha_3|0\rangle_L + \alpha_4|1\rangle_L = \alpha_3|0\rangle_3|1\rangle_4 + \alpha_4|1\rangle_3|0\rangle_4 \quad (32)$$

It's crucial to highlight the influence of the first beam splitter: when both qubits are in state $|1\rangle$, modes 1 and 3 are in the state $|11\rangle_{13}$, which transforms to $|20\rangle_{13} + |02\rangle_{13}$. In none of the other cases do two photons appear in the same mode. Thus both NSs have the desired effect. Because both of these operations must succeed, c-$z_{1/16}$ succeeds with probability 1/16, [17].

A CNOT gate can be constructed from two NS gates as shown schematically in Fig. 12). Here the control and target qubits are encoded in optical mode or path ("dual-rail encoding"), with a photon in the top mode representing a logical 0 and in the bottom a logical 1. The target modes are combined at a 1⁄2 reflectivity BS (BS3), interact with the control 1 mode via the central Mach-Zehnder interferometer (MZ) physics, and are combined again at a 1⁄2 reflectivity BS (BS4) to form another MZ physics with the two target modes, whose relative phase is balanced such that, in the absence of a control photon, the output state of the target photon is the same as the input state. The goal is to impart a π phase shift in the upper path of the target MZ physics, conditional on the control photon being in the 1 state such that the NOT operation will be implemented on the target qubit. When the control input is 1, quantum interference between the control and target photons occurs at BS1: $|1\rangle_{C_1}|1\rangle_{T_0} \rightarrow |2\rangle_{C_1}|0\rangle_{T_0}$. In this case the NS gates each impart a π phase shift to these two-photon components: $|2\rangle_{C_1/T_0} \rightarrow -|2\rangle_{C_1/T_0}$. At BS2 the reverse quantum interference process occurs, separating the photons into the C_1 and T_0 modes, while preserving the phase shift that was implemented by the NS gates. In this way the required π phase shift is applied to the upper path of the target MZ, and so CNOT operation is realized, [32].

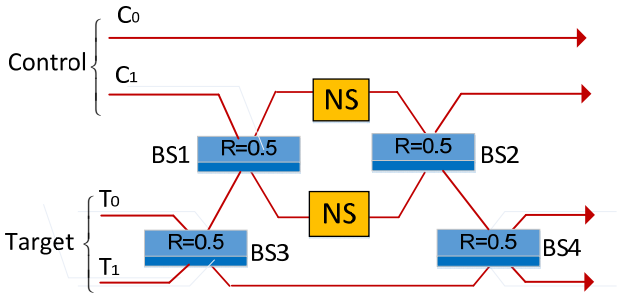

Fig. 12 The KLM CNOT gate. The gate is constructed of two NS gates; the output is accepted only if the correct heralding signal is observed for each NS gate. Gray indicates the surface of the BS from which a sign change occurs upon reflection. Adapted from [32]

5. CONCLUSIONS

Main methods of optical qubit implementations are polarization and path encoding, but, also, other methods like transverse spatial mode, frequency mode, temporal bin-mode, and temporal mode encoding, are under consideration. Transverse spatial mode, frequency mode, and temporal mode enable implementation of qudits, meaning more efficient computation.

Linear optical quantum computing is capable of implementing any single qubit gate by using only beam splitters and phase shifters. It is also capable of implementing two qubit gates like c-$z_{1/16}$ and CNOT gate by using beam splitters, phase shifters, single-photon sources, and single-photon detectors.

The fact that linear optical quantum computing can implementing any single qubit gate and CNOT gate means that linear optical quantum computing can implement any quantum mechanical gate, [13].

REFERENCE

[1] Bhat H. A. , Khanday F.A., Kaushik B. K., Bashir F., Shah K.A. Quantum Computing: Fundamentals, Implementations and Applications, *IEEE Open Journal of Nanotechnology,* 2022, 3, 61-77.

[2] Krovi H. Models of optical quantum computing, *Nanophotonics* 2017; *6(3),* 531–541

[3] O'Brien, J. L. Optical Quantum Computing, *Science*, 2008, Vol. 318, No. 5856, 1567-1570.

[4] Ralph T.C., Pryde G.J. Optical Quantum Computation, In: E.Wolf (Ed.), *Progress in Optics,* 2009, 54, Elsevier, New York, pp. 209-263.

[5] Hong C., Ou Z.-Y. & Mandel L. Measurement of subpicosecond time intervals between two photons by interference. *Physical review letter*. 1987, 59(18), 2044-2046.

[6] Giustina M. et al. Significant-loophole-free test of bell's theorem with entangled photons, *Physical review letter,* 2015, 115, 250401 (7pp).

[7] Shalm L. K. et al. Strong loophole-free test of local realism, *Physical review letter,* 2015, 115, 250402 (10pp).

[8] Cai X.-D. et al. Experimental quantum computing to solve systems of linear equations, *Physical review letter,* 2013, 110, 230501(5pp).
[9] Barz S. et al. A two-qubit photonic quantum processor and its application to solving systems of linear equations, *Scientific Reports,* 2014, 4, 6115 (6pp).
[10] Azuma K., Tamaki K., Lo, H.-K. All-photonic quantum repeaters. *Nature Communications,* 2015, 6, 6787 (7pp).
[11] Zeuner J. et al. Integrated-optics heralded controlled-NOT gate for polarization-encoded qubits, *npj Quantum Information,* 2018, 13, 1-6, doi:10.1038/s41534-018-0068-0.
[12] Pittman T. B., Jacobs B. C. and Franson J. D. Quantum Computing Using Linear Optics, *Johns Hopkins APL technical digest,* 2004, Vol. 25, No. 2, 84-90
[13] Nielsen M., Chuang I. *Quantum Computation and Quantum Information*. Cambridge University Press, New York, 2010.
[14] Chubb J., Harizanov V. A. (Very) brief tour of quantum mechanics, computation, and category theory**,** In *Logic and Algebraic Structures in Quantum Computing,* 2016, 8-22, Cambridge University Press, United Kingdom.
[15] Brecht B., Reddy D. V., Silberhorn C., Rayme M. G. Photon Temporal Modes: A Complete Framework for Quantum Information Science, *Physical Review,* 2015, *X 5*, 041017 (17pp).
[16] Knill E. Quantum gates using linear optics and postselection, *Physical Review* 2002, *A 66 (5),* 052306 (5pp).
[17] Knill E., Laflamme R., Milburn G. J. A scheme for efficient quantum computation with linear optics. *Nature,* 2001, 409*, 46–52.*
[18] Drahi D. et al. Entangled resource for interfacing single- and dual-rail optical qubits, *Quantum,* 2021, 5, 416 (9pp).
[19] Pittman T. B., Jacobs B. C., Franson J. D. Quantum Computing Using Linear Optics*, Johns Hopkins APL technical digest,* 2004, Vol. 25, No. 2, 84-90
[20] Wang J.and Liang Y. Generation and Detection of Structured Light: A Review. *Frontiers in Physics,* 2021, Vol. 9, Article 688284 (16pp).
[21] Erhard M., Fickler R., Krenn M., Zeilinger A. Twisted photons: new quantum perspectives in high dimensions, *Light: Science & Applications,* 2018, 7, 17146 (11pp).
[22] Hiekkamäki M., Prabhakar S., Fickler R. Near-perfect measuring of full-field transverse-spatial modes of light, *Optics Express,* 2019, Vol. 27, No. 22, 31456-31464.
[23] Raymer M. G., Walmsley I. A. Temporal modes in quantum optics then and now, *Phys. Scr.,* 2020, 95, 064002 (17pp).
[24] Lukens J. M. and Lougovski. P. Frequency-encoded photonic qubits for scalable quantum information processing, Optica, 2017, Vol. 4, No. 1 , 8-16
[25] Pittman T. B., Jacobs B. C., Franson J. D. Quantum Computing Using Linear Optics*, Johns Hopkins APL technical digest,* 2004, Vol. 25, No. 2, 84-90.
[26] Agarwal G.S. Quantum Optics; Cambridge University Press: Cambridge, UK; p. 491. 2013.
[27] Zeilinger A. General properties of lossless beam splitters in interferometry. *American Journal of Physics*, 1981, 49(9), 882–883, doi:10.1119/1.12387.
[28] Campos A. R., Saleh E. A. B. and Teich C. M. Quantum-mechanical lossless beam splitter: SU(2) symmetry and photon statistics, *Physical Review*, 1989, A, Vol. 40, No. 3, 1371-1384.
[29] Luis A., Sfinchez-Soto L. AQuantum description of the beam splitter. *Quantum Semiclass. Opt.*, 1995. 7, 153–160.
[30] Titulaer U., Glauber R. Density Operators for Coherent Fields. *Physical Review*, 1966, 145, 1041-1049.
[31] Amoroso R. L. Universal quantum computing: supervening decoherence — surmounting uncertainty. World Scientific, Hackensack. 2017.
[32] Okamoto R., O'Brienc J. L., Holger F. H., Takeuchi S. Realization of a Knill-Laflamme-Milburn controlled NOT photonic quantum circuit combining effective optical nonlinearities, PNAS, 2011, Vol. 108, No. 25, 10067–10071.